Field Testing a Mobile Inelastic Neutron Scattering System to Measure Soil Carbon

Galina Yakubova,[1] Lucian Wielopolski,[2] Aleksandr Kavetskiy,[1] H. Allen Torbert,[1] and Stephen A. Prior[1]

Abstract: Cropping history in conjunction with soil management practices can have a major impact on the amount of organic carbon stored in soil. Current methods of assessing soil carbon based on soil coring and subsequent processing procedures before laboratory analysis are labor intensive and time-consuming. Development of alternative methods that can make *in situ* field measurements of soil carbon is needed to successfully evaluate management practices in a timely manner. The robust design, field testing procedure, and results of measuring soil carbon *in situ* using a mobile inelastic neutron scattering (MINS) system are described. A method of MINS spectra data processing that gives more accurate peak area determination compared with the traditional "trapezoidal" method is described. The MINS reliable autonomous operation for 29 h per charge cycle was demonstrated in the field. For comparison, soil cores were also collected for laboratory carbon analysis using the dry combustion technique. Soil carbon assessments by dry combustion technique and MINS demonstrated a linear correlation between the two methods in the 0- to 30-cm soil layer. Based on the developed theoretical model of MINS measurement, we demonstrated that accurate soil carbon determination by this method depends on carbon distribution within the soil and MINS signal errors.

Key Words: Carbon, soil analysis, inelastic neutron scattering, thermo-neutron capture, neutron generator

(*Soil Sci* 2014;179: 529–535)

The acceptance of agricultural land use practices that adapt to climate change pressures and potentially mitigate global impacts depends on the productivity and profitability of agricultural operations. The development of sustainable land use practices requires understanding and evaluating the impacts of these practices on soil resources. Measurement and mapping of natural and anthropogenic variations in soil carbon stores is a critical component of any soil resource evaluation process. The current state-of-the-art method to determine soil carbon content is based on the dry combustion technique (DCT) (Nelson and Sommers, 1996). This method is destructive, time-consuming, and labor intensive because it not only entails collecting numerous soil core samples in the field but also requires extensive sample preparation before complex laboratory analysis. In addition, the information gained from DCT soil analysis represents a point measurement in space and time that creates uncertainty when extrapolating to field or landscape scale, thereby limiting its utility for expansive coverage or longer timescale interpretation.

[1]U.S. Department of Agriculture–Agricultural Research Service National Soil Dynamics Laboratory, Auburn, Alabama, USA.
[2]Brookhaven National Laboratory, Environmental Sciences Department, Upton, New York, USA.
Address for correspondence: Dr. Galina Yakubova, USDA-ARS National Soil Dynamics Laboratory, 411 South Donahue Dr, Auburn, AL 36832, USA. E-mail: galina.yakubova@ars.usda.gov
Financial Disclosures/Conflicts of Interest: *None reported*.
Received August 4, 2014.
Accepted for publication December 29, 2014.

ISSN: 0038-075X
DOI: 10.1097/SS.0000000000000099

A new methodology using soil neutron-activation analysis provides the possibility of measuring soil carbon content over relatively large soil volumes without requiring soil sample collection and processing via typical laboratory analysis. Our alternative method is based on soil irradiation by fast neutron flux and subsequent measurement of the gamma response. One modification of this method, the inelastic neutron scattering (INS) technique, has been demonstrated to be an integrating approach that can provide wide-area monitoring for prolonged periods (Wielopolski et al., 2008, 2011). The estimated minimum detectable limit of carbon content to a depth 0 to 30 cm for the INS technique is approximately 0.23 kg C m^{-2} (~0.023 g C cm^{-2}), which is approximately 3.5% of the current soil carbon content (Wielopolski et al., 2010). Although this limit is better than the DCT methodology, the INS methodology has not been fully developed for large-scale use.

The objective of this study was to incorporate INS technology into mobile equipment suitable for field measurements. The present article describes the INS equipment developed for routine soil measurements, details a new method of mobile INS (MINS) spectra data processing that gives more accurate peak area determination compared with the traditional "trapezoidal" method (Ramirez and Wielopolski, 2004), compares INS field measurements of soil carbon with the standard DCT method, and analyzes the effect of soil carbon distribution on INS measurements.

MATERIALS AND METHODS

Field Description and Soil Sampling

For field testing the MINS, five experimental plots were established at the Alabama Agricultural Experiment Station Piedmont Research Unit, Camp Hill, Alabama. This area was selected because it had a uniform treatment history during the long-term (i.e., held in pasture for >40 years) and was fairly close in proximity to our facility at the National Soil Dynamics Laboratory in Auburn, Alabama. Furthermore, being located at the experiment station allowed for study oversight and use of available farm equipment required to conduct the experiment. The study was conducted on a Cecil sandy loam (fine, kaolinitic, thermic typic Kanhapludults); the climate is humid subtropical with an average annual precipitation of approximately 1,100 mm. Four plots measuring 8 × 32 m each were subjected to various plowing depth treatments (i.e., AF1–AF4; Fig. 1). The AF1 plot was plowed to a depth of 30 cm (moldboard plow), AF2 was plowed to 15 cm (breaking harrow), AF3 was plowed to 10 cm (smoothing harrow), and AF4 was no-tillage. A fifth plot was an unplowed 32 × 110–m open field (OF) (Fig. 1). The numbered points shown in the figure were locations where soil carbon was measured by MINS and DCT. An indoor sand bin (6 × 6 m) was also used in the development of the MINS analysis equation. Two soil pits (1.5 × 1.5 m) containing pure sand and a mixture of the sand and granular carbon (~10% by weight), located at Brookhaven National Laboratory, were also used for checking the workability of MINS. Because of the extremely rough surface generated by deep plowing in the AF1 location, both the MINS and DCT

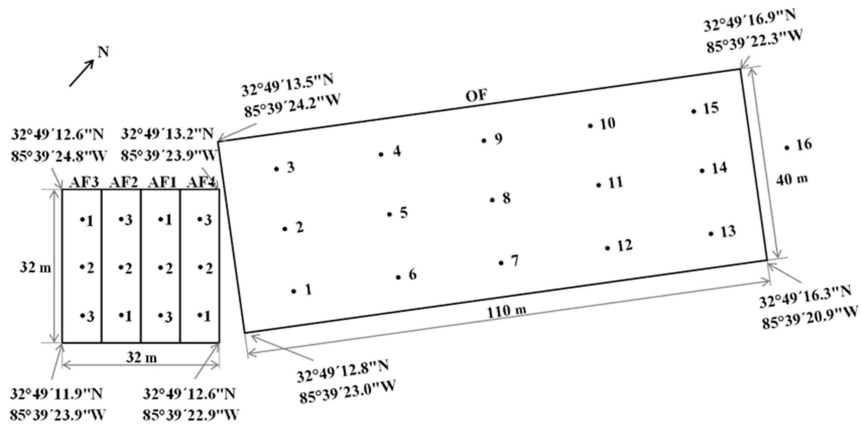

FIG. 1. Field study site schematic: AF1 = 30 cm plowing depth; AF2 = 15 cm plowing depth; AF3 = 10 cm plowing depth; AF4 = no-tillage; and OF = open field (no tillage). Each dot located adjacent to numbers represents a sampling point in the study.

measurements were very different from measurements at others locations and were, therefore, not included in this research.

A depth profile of soil carbon measured at each site was determined by DCT for site characterization. Three to five cores (4 cm in diameter × 100 cm in length) were taken from a 30 × 30–cm area around the center of each sampling position. All cores were collected using a tractor-mounted hydraulic system previously described by Prior et al. (2004). All cores were divided into 10-cm increments, sieved (2 mm), and oven-dried at 55°C until constant weight. Soil bulk density (ρ_s, g cm^{-3}) for each 10-cm depth segment was determined using standard methods (Blake and Hartge, 1986). Subsamples were ground with a roller grinder (Kelley, 1994) and analyzed by DCT using a LECO TruSpec CN analyzer (LECO Corp., Saint Joseph, MI) to determine soil carbon concentration in percent by weight (C_{cw}, %). The carbon content (Cc, g C cm^{-3}) for each portion was calculated as $Cc = \rho_s \cdot C_{cw}/100\%$.

The distribution of carbon content with depth was described by an exponential function in accordance with a previously published model (Wielopolski et al., 2008):

$$Cc(d) = c + a \exp(-b\,d) \quad (1)$$

where c is a constant component of carbon content in soil (g C cm^{-3}); a and b define the dynamic change of carbon in soil (g C cm^{-3} and cm^{-1}, respectively); and d is depth (cm).

The MINS measures the average carbon content in the upper soil layer to a depth of approximately 30 cm (Wielopolski et al., 2008). The carbon content in this layer was characterized by the carbon surface content (Csc, gC cm^{-2}) of the 0- to 30-cm soil layer. Dependencies of Csc with depth for each site can be derived by integration of the carbon content depth profile given by Eq.(1). This function is expressed by Eq.(2):

$$Cc(d) = c\,d + \frac{a}{b}(1 - \exp(-b\,d)) \quad (2)$$

Eq.(2) was used for calculation of the carbon surface content at each site.

MINS System

The MINS system was designed to operate on a platform that can be maneuvered by tractors or all-terrain vehicles over any type of field terrain-requiring measurement. The mobile platform has dimensions of 75 × 23 × 95 cm and weighs approximately 300 kg; whereas aluminum was the primary construction material, lead shielding adds considerably more weight. Previous findings from Brookhaven National Laboratory (Wielopolski et al., 2008, 2010) were used to facilitate the physical construction and electronic requirements of this system. The MINS system consisted of three separate construction blocks (Fig. 2). The first block contained an MP320 neutron generator (Thermo Fisher Scientific, Colorado Springs, CO), an R2D-410 neutron detector (Bridgeport Instruments, LLC, Austin, TX), and the power system (Fig. 2A, D). The neutron generator produced a pulsed output of 10^7 to 10^8 n s^{-1} depending on parameter settings; neutron energy is 14 MeV. The MINS power system consisted of four DC105-12 batteries (12V, 105Ah), a DC-AC inverter (CGL 600W-series; Nova Electric, Bergenfield, NJ), and a Quad Pro Charger model PS4 (PRO Charging Systems, LLC, LaVergne, TN). This block also consisted of lead shielding to isolate the neutron beam and focus it on the soil area to be measured. The second block consisted of gamma ray–measuring equipment (Fig. 2B, E). This block contained three 12.7 × 12.7 × 15.2–cm scintillation NaI(Tl) detectors (Scionix USA, Orlando, FL) with corresponding XIA LLC electronics (XIA LLC, Hayward, CA). The third block (Fig. 2C) was for equipment operation by a laptop computer that controls the neutron generator, detectors, and the data acquisition system ProSpect 0.1 (XIA LLC) (Fig. 2C).

In the applied INS technique, gamma rays emitted by soil chemical elements under pulsed neutron irradiation can be divided into two main groups: those emitted during neutron pulse because of INS and thermo-neutron capture (TNC) and those emitted between neutron pulses because of TNC reaction. Also, delay gamma rays (i.e., caused by neutron activation reactions) were present in these spectra. With each MINS measurement, the two gamma spectra that were concurrently acquired by the detectors (i.e., INS and TNC spectra) were treated together (Wielopolski et al., 2000).

Spectra acquisition from the three gamma detectors can be collected in two separate ways. First, analog signals from the detectors went to a summing amplifier and were then processed by a digital multichannel analyzer (Mitra et al., 2007). Second, each detector had its own analog-digital converter to acquire spectra; these were summarized after correction for energy calibration instability (Wielopolski et al., 2010; Tan et al., 2008). During testing, the second method demonstrated improved resolution in the measurement system and was therefore adopted for use in MINS.

For the MINS system to operate autonomously under field conditions, a mobile power system that could reliably operate all equipment for extended periods was developed. In the MINS, the neutron generator, neutron and gamma detectors, and laptop

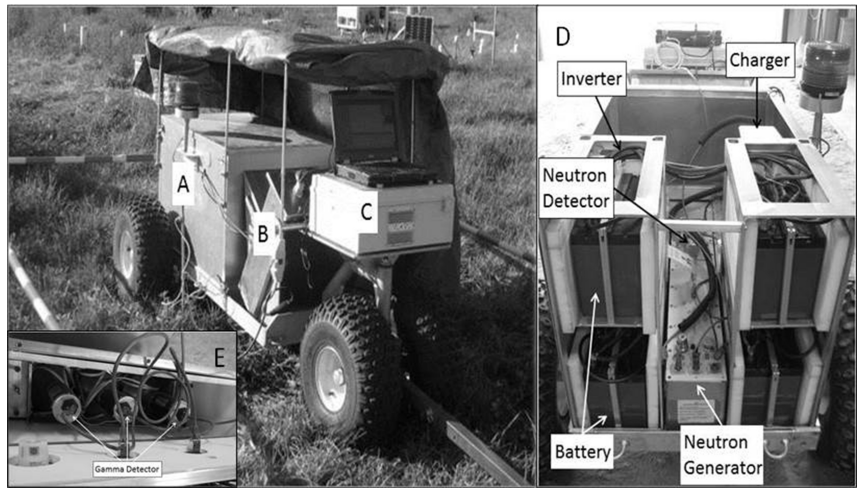

FIG. 2. Overview of the MINS: (A) neutron generator, neutron detector, and power system; (B) three NaI (Tl) detectors; (C) equipment operation; (D) general view of A showing individual components; and (E) close-up view of the gamma detectors.

computer were all powered by four batteries through the inverter. The inverter transformed 12 V of direct current battery power to 110 V alternating current. The inverter operated at input voltages varying from 10.9 to 14.7 V.

Method of Spectra Analysis

There are two gamma spectra for each MINS measurement: INS and TNC. In Fig. 3, typical gamma spectra from soil (raw spectra) during system testing are shown by solid and dotted lines, respectively. Each spectrum consists of background levels and gamma ray measurement lines that are emitted by chemical elements in the soil under neutron irradiation. The main gamma peak of interest was the peak with a centroid at 4.43 MeV in the INS spectrum. The peak seems caused by the neutron interaction with carbon nuclei and interference of gamma lines from the silicon nuclei (Wielopolski et al., 2008). The oxygen peak (6.13 MeV) and the pair production peak (0.511 MeV) were used as reference points for correction of the whole spectrum because of possible shifting during any given set of measurements.

Analysis of each spectrum was conducted in two steps. First, the background was fitted and subtracted from the raw spectrum to provide a net spectrum. Second, the areas under the peaks of interest were calculated using the appropriate Gaussians that fit these peaks.

Assuming that the background was caused by the Compton Scattering (Knoll, 2000) and multi–gamma lines with small yield, it can be considered as continuous (Batdorf et al., 2009; East et al., 1982) and can be approximated by a smooth curve. For this, the whole energy scale (0–8 MeV) was divided into three regions, and the background at each region was fitted by a double exponential function. Border fitted points for adjusted regions were chosen in a similar fashion with a smooth transition between them. Examples of fitting using this method are shown by the dashed curves in Fig. 3.

Examples of net spectra are shown in Fig. 4. In this figure, three spectra are plotted: (i) over a sand pit, (ii) over a "carbon" pit (mixture of sand and ~10% by weight of granular carbon), and (iii) one of the field points (OF-1). Measurements conducted over sand and carbon pits were used to check the workability of MINS.

The main gamma peak of interest (i.e., centroid 4.43 MeV) from sand and carbon pits and OF-1 point are shown in the inset of Fig. 4. As can be seen, the peaks for the carbon pit and OF-1 spectra are higher than the sand pit spectrum because of the

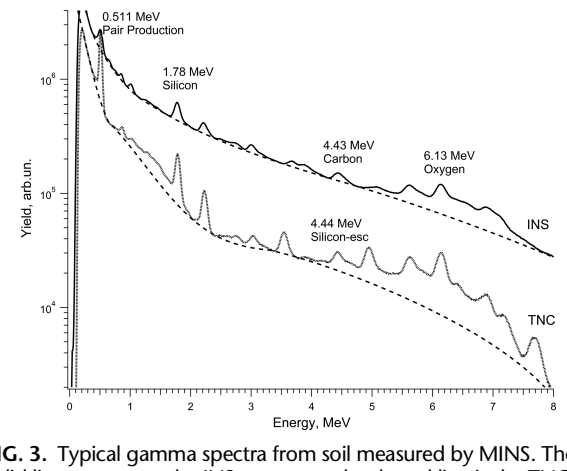

FIG. 3. Typical gamma spectra from soil measured by MINS. The solid line represents the INS spectrum, the dotted line is the TNC spectrum, and the dashed lines are the background fitting.

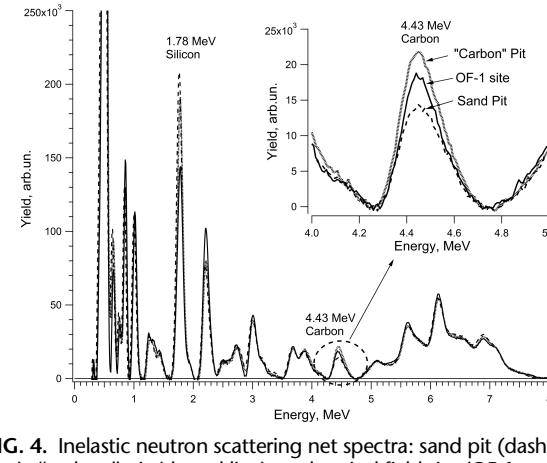

FIG. 4. Inelastic neutron scattering net spectra: sand pit (dashed line), "carbon" pit (dotted line), and typical field site (OF-1, solid line); peak with centroid at 4.43 MeV for the field site (OF-1) and the "carbon" and sand pits is shown in the insert.

carbon component, demonstrating that MINS can measure carbon in the field.

The net areas of these peaks were calculated by Gaussian fitting using IGOR software (WaveMetrics Inc., Portland, OR). To refine the value of the 4.43 MeV peak area defined particularly by carbon in soil, deconvolution for extracting the carbon peak was conducted. Silicon peaks (1.78 MeV in INS and TNC and 4.44 MeV in TNC spectra) were used for this correction. The carbon peak area that is caused by carbon nuclei only (C) is the part of the peak with a centroid of 4.43 MeV and is calculated as (Wielopolski et al., 2008):

$$C = C_p - Si_{TNC}(4.44)\,LT_{INS}/LT_{TNC} - [Si_{INS}(1.78) - Si_{TNC}(1.78)\,LT_{INS}/LT_{TNC}]\,k \quad (3)$$

where C_P is the peak area with centroid 4.43 MeV, Si_{TNC} (4.44) is the silicon escape peak area with energy 4.44 MeV in TNC spectrum, Si_{INS} (1.78) is the silicon peak area with energy 1.78 MeV in the INS spectrum, Si_{TNC} (1.78) is the silicon peak area with energy 1.78 MeV in the TNC spectrum, LT_{INS} and LT_{TNC} are acquisition life times for the INS and TNC spectra, and k is the coefficient defining the relationship of transmission probability in silicon nuclei. Coefficient k was calculated to be 0.175 by setting Eq. (3) equal to zero and inputting the carbon peak area from the sand bin.

Accuracy of the INS Measurements

The accuracy of carbon surface content measured with the current approach of MINS depends on different factors. It was found (see below) that main factors affecting the accuracy are MINS measurement errors (Δ_{total}) and errors caused by variation of carbon distribution in soil (Δ_{var}). Thus, a first approximation of measured carbon surface content accuracy could be estimated as:

$$\Delta_{MINS} = \sqrt{\Delta^2_{total} + \Delta^2_{var}} \quad (4)$$

Theoretical Model of Gamma Ray Yield in INS Measurements

Analysis shows that variation in soil carbon distribution affects the carbon-associated gamma peak. To theoretically estimate the effect of this variation, a mathematical model was developed to characterize the influence of soil carbon distribution on the 4.43 MeV gamma detector signal (Appendix 1).

That model allows for estimating the dependence of the gamma detector yield with different soil parameters (e.g., weight percent of various nuclei, soil density, thickness of the soil layer, etc.). The calculation can be made using appropriate software such as Mathcad (MathSoft Inc., Cambridge, MA). As a first approximation, a synthetic soil consisting of carbon and sand (SiO_2) can be used to analyze the effects of different soil parameters on the gamma detector signal. To use the model, the dependencies of weight percent and soil density with depth and the total macroscopic cross section of neutrons interacting with soil nuclei and the linear attenuation coefficient of 4.43 MeV gamma rays in soil should be known. In describing carbon distribution with depth, the dependencies of weight percent and soil density with depth can be built as stepped functions using 10-cm increments where parameter values for each step are the average values for the site at this depth based on DCT measurements. The total macroscopic cross section of neutrons interacting with soil nucleus and the linear attenuation coefficient of 4.43 MeV gamma rays in soil for each step was calculated as described in Appendix 1.

RESULTS AND DISCUSSION

Power Requirement Testing

As part of the developmental process, the MINS autonomous working time was defined in laboratory conditions. For testing purposes, the system was ran for background measurement and an equivalent external load (1.4 A) was used to simulate the current draw of the neutron generator. The time of autonomous work was approximately 29 h. That autonomous working time was verified during field testing.

Analysis of DCT Measurements

The dependencies of experimental soil carbon content (Cc) with depth (depth profile) were examined for each core. For each site, the average carbon value was determined from values of Cc (i.e., from three to five core segments per depth) and the dependence of this average Cc value with depth was also plotted. For example, the dependencies at the OF-8 site are shown in Fig. 5. As can be observed, some experimental points are outside the prediction band for the average site values. This was likely the result of local carbon enrichment of an individual sample caused by small pieces of organic material (e.g., root and/or other organic residue fragments) in the soil sample. These small organic components do not have a practical effect on the MINS measurement because the system measures average carbon content of a relatively large soil volume (~0.3 m^3) to a depth of approximately 30 cm (Wielopolski et al., 2010); results would include these organic components but would not be sensitive to these small point variations under the MINS footprint. In contrast, DCT measurements can be very sensitive to the presence of point variations, potentially resulting in big deviations from the real average value, thereby distorting the true average depth profile description. Such distortion can skew comparisons of MINS and DCT results. To avoid this distortion, depth profile was recalculated (i.e., solid line in Fig. 5) without the data that fell outside the prediction band for the average. For the corrected depth profile, the regression coefficients c, a, and b (Eq.(1)) with corresponding errors were determined. The same depth profile data analysis was done for each site, and the corrected profile was used for comparison with MINS data. Values of the fitted parameters varied in the range of 0.0008 to 0.0084 g C cm^{-3} for c, 0.014 to 0.072 g C cm^{-3} for a, and 0.062 to 0.206 cm^{-1} for b.

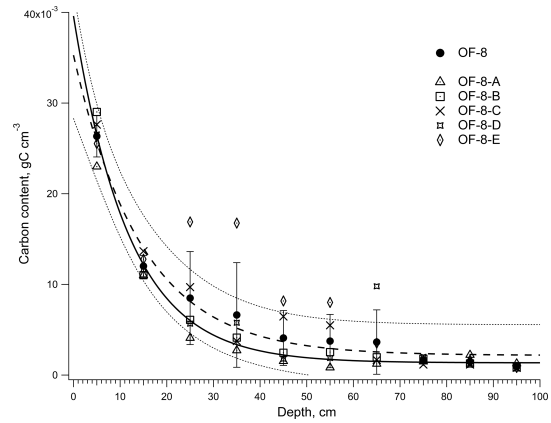

FIG. 5. Carbon content depth profile for the OF-8 site. Symbols represent the experimental data for five soil cores labeled A to E: solid circles with error bars are the average data for five cores; dashed line is the fitting function; dotted lines are the prediction band; and the solid line is the corrected fitting function.

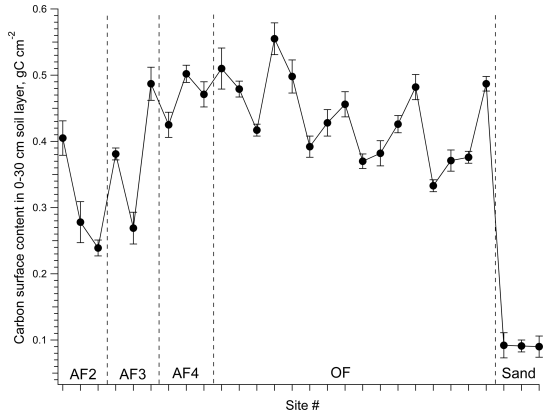

FIG. 6. Site-to-site variation of carbon surface content in the 0- to 30-cm soil layer; points are *Csc*(30 cm) derived from Eq.(2), whereas error bars were calculated from the prediction bands.

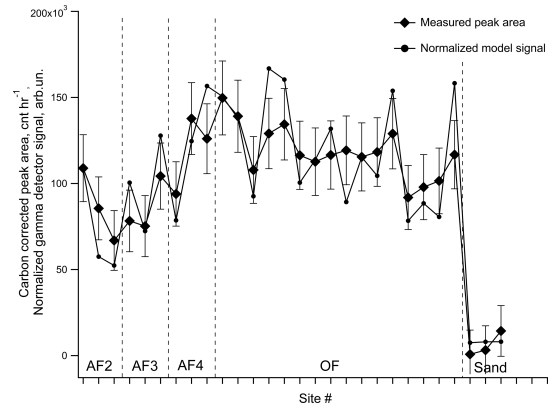

FIG. 8. Site-to-site variation of the measured carbon corrected peak area (rhomb) and calculation by model-normalized 4.43-MeV gamma detector signal (points).

The carbon content in the upper soil layer was characterized by the carbon surface content (*Csc*, g C cm^{-2}) of the 0- to 30-cm soil layer. The values of *Csc*(30) for each site was calculated by Eq.(2). The *Csc* range variation at the 30-cm depth with error bars (95% confidence level) for all sites is shown in Fig. 6. Error bars were calculated from the prediction band for *Csc*(30) for each particular sampling location. The figure shows that the *Csc*(30) for fields varied from approximately 0.2 to 0.6 g C cm^{-2}.

Analysis of MINS Field Measurements

The MINS measurements were conducted for each site (Fig. 1) for 1 h, processed as previously described, and the results were used to determine the correlation of MINS with DCT measurements. The values of the carbon-corrected peak areas calculated by Eq.(3) based on MINS measurements for the field measured sites are shown in Fig. 7 versus carbon surface content. There was a direct correlation between MINS results and carbon surface content as determined by DCT analysis. The coefficient of determination (r^2) for this relationship was 0.89 (at a 95% confidence level). Therefore, according to the given regression equation, 89% of the data showed a linear relationship between the standard soil carbon measurement technique and MINS. The prediction band is defined by dispersion of the measured points around the regression line and gives the error in determination of carbon surface content (Δ_{var}) equal to approximately 0.09 g C cm^{-2}.

The dispersion of the MINS results around the regression line could have two causes: measurement error and variation of carbon distribution in soil. To understand this dispersion, the values of the 4.43 MeV gamma detector signal for each site, based on the theoretical model using Eq.(5A), were calculated (see Appendix 1). It was found that the ratios of these values to the measured corrected carbon peak area occasionally vary from the average ratio value within the limits of ±19%. The model calculated values were normalized by dividing by this average value. The measured and normalized model values are shown in Fig. 8. As can be seen, the measured and normalized model values are very close to each other for practically all sites. Thus, it seems that the developed theoretical model successfully describes the 4.43-MeV gamma detector signals associated with soil carbon content and can be used to analyze the effects of different factors on the value of the INS signal.

The model-calculated values for 4.43-MeV gamma detector signals of carbon surface content in the 0- to 30-cm soil layer are shown in Fig. 9 by points. This dependence can be approximated by a straight line. The calculated points lie inside the prediction band (95% confidence level) denoted on this plot and were determined by variation in carbon distribution at the sites.

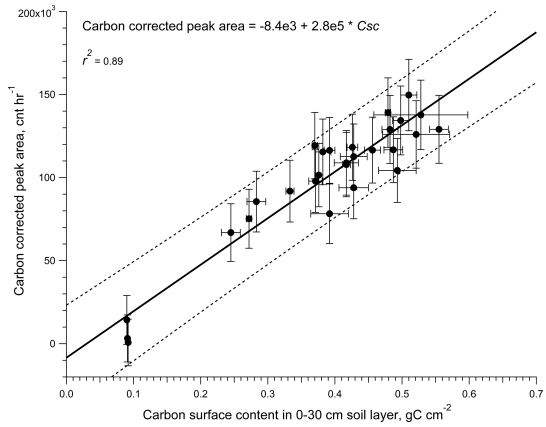

FIG. 7. The dependence of the MINS measurements with DCT analysis results for the 0- to 30-cm soil layer. Points with 95% error bars for both coordinates are experimental results; solid line is a regression line; and dashed lines are the prediction band.

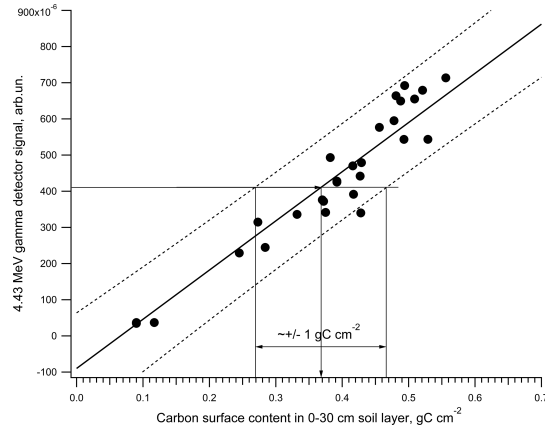

FIG. 9. The dependence of the model-calculated 4.43-MeV gamma detector signal with DCT analysis results for the 0- to 30-cm soil layer. Points are the model-calculated values; solid line is a regression line; and dashed lines are the prediction band.

The error of carbon surface content measurements caused by varying site-to-site carbon distribution was ±0.1 g C cm^{-2} (Fig. 9).

The theoretical calculated variations of the 4.43-MeV gamma detector signals caused by variation in soil carbon distribution and measured dispersion of MINS results were very close and therefore can be assumed to be caused by variation of carbon distribution from site to site. This variation should be taken into ac count when estimating the accuracy of soil carbon content determination by MINS together with error of the MINS measurements.

Statistical analysis of MINS measurement error showed that variation of the peak area caused by inaccuracy of background fitting was 5% (i.e., ~$5 \cdot 10^3$ counts with a 95% confidence level); this value was taken as the system error (Δ_{sys}). The statistical error (Δ_{st}) was composed of errors from all components in Eq.(3); however, error of the carbon peak area in the INS spectrum is an order of value larger than other error components in the equation. Thus, the statistical error was taken from the results of Gaussian fitting of the carbon peak in the INS spectrum (i.e., Δ_{st} ~$1.5 \cdot 10^4$ counts with a 95% confidence level). Total error (Δ_{total}) was estimated as the sum of system and statistical errors (i.e., ~$2 \cdot 10^4$ counts with a 95% confidence level). Carbon content in soil was determined from MINS measurements by a reverse regression equation. Total error of each carbon content measurement (g C cm^{-2}) is Δ_{total} divided by the slope of the regression line (Fig. 7) and can be estimated as approximately $2 \cdot 10^4 / 2.8 \cdot 10^5 = 0.07$ g C cm^{-2}.

The accuracy of carbon surface content measured with the current approach of MINS (Δ_{MINS}) for the 0- to 30-cm soil layer (95% confidence level) could be estimated from the error of MINS measurements (Δ_{total} = 0.07 g C cm^{-2}) and error caused by varying carbon distribution in soil (Δ_{var} = 0.09 g C cm^{-2}) by Eq.(4), such that Δ_{MINS} = 0.12 gC cm^{-2}.

The sensitivity (s) of MINS to *Csc* was described by the slope of the regression line in Fig. 7 and was equal to $2.8 \cdot 10^5$ cnt h^{-1} g C^{-1} cm^2 (or $2.8 \cdot 10^4$ cnt h^{-1} kg C^{-1} m^2). The minimum detectable limit defined by the equation $MDL = 3\sqrt{B}/s$ (B is background under the peak with centroid 4.43 MeV in the raw spectrum; Wielopolski et al., 2010) was approximately 0.03 g C cm^{-2}.

CONCLUSIONS

A number of major points can be made based on the results of the present study. First of all, field testing demonstrated reliable autonomous work of MINS. All MINS measurements were completed at 28 sites during a 4-day period (4–14 h/d); this represents a large time savings relative to the DCT approach. Carbon surface content from the 0- to 30-cm soil layer defined by chemical analysis (DCT) and MINS results indicated a linear correlation between the two methods. The carbon sensitivity of MINS was equal to $2.8 \cdot 10^5$ cnt·h^{-1}·g C^{-1}·cm^2. The minimum detectable limit for MINS was approximately 0.03 g C cm^{-2}. The accuracy of carbon surface content for 30-cm soil depth was ±0.12 g C cm^{-2}. This accuracy is a result of two main factors: accuracy of the MINS signal (0.07 g C cm^{-2}) and variation of soil carbon distribution (0.09 g C cm^{-2}). The MINS field testing demonstrated that this system could determine soil carbon content under field conditions without the need of standard laboratory soil analysis.

ACKNOWLEDGMENTS

The authors thank Barry G. Dorman, Robert A. Icenogle, and Morris G. Welch for technical assistance in collecting and processing soil samples. The authors thank XIA LLC for allowing the use of their electronics and detectors in this project. The authors also acknowledge Dr. Sudeep Mitra's invaluable advice and support during this project.

REFERENCES

Batdorf M. T., W. K. Hensley, C. E. Seifert, L. J. Kirihara, L. E. Erikson, and D. V. Jordan. 2009. Isotope identification in the gamma tracker handheld radioisotope identifier. IEEE Nucl. Sci. Symp. Conf. Rec. (NSS/MIC) 868–872.

Blake G. R., and K. H. Hartge. 1986. Bulk density. *In*: Methods of Soil Analysis: Part 1. Physical and Mineralogical Methods. Agronomy Monograph No. 9. 2nd Ed. Klute A. (ed.). ASA and SSSA, Madison, WI, 363–375.

East L. V., R. L. Phillips, and A. R. Strong. 1982. A fresh approach to NaI scintillation detector spectrum analysis. Nucl. Instr. Methods. 193:147–155.

Knoll G. F. 2000. Radiation Detection and Measurement. (3rd ed.) Inc, John Willey & Sons: New York.

Kelley K. R. 1994. Conveyor-belt apparatus for fine grinding of soil and plant materials. Soil Sci. Soc. Am. J. 58:144–146.

Mitra S., L. Wielopolski, H. Tan, A. Fallu-Labruyere, W. Hennig, and W. K. Warburton. 2007. Concurrent measurement of individual gamma-ray spectra during and between fast neutron pulses. Nucl. Sci. 54:192–196.

National Institute of Standards and Technology. 2004. X-ray mass attenuation coefficients. at: http://physics.nist.gov/PhysRefData/XrayMassCoef/tab1.html.

National Nuclear Data Center, Brookhaven National Laboratory. 2013. Available at: http://www.nndc.bnl.gov/sigma/index.jsp.

Nelson D. W., and L. E. Sommers. 1996. Total carbon, organic carbon, and organic matter. *In*: Methods of Soil Analysis, Part 3, Chemical Methods. Sparks D. L. (ed.). SSSA and ASA, Madison, WI, 961–1010.

Prior S. A., G. B. Runion, H. A. Torbert, and D. C. Erbach. 2004. A hydraulic coring system for soil-root studies. Agron. J. 96:1202–1205.

Ramirez L. M., and L. Wielopolski. 2004. Analysis of potassium spectra with low counting statistics using trapezoidal and library least-squares methods. Appl. Radiat. Isot. 61:1367–1373.

Tan H., S. Mitra, L. Wielopolski, A. Fallu-Labruyere, W. Hennig, Y. X. Chu, and W. K. Warburton. 2008. A multiple time-gated system for pulsed digital gamma-ray spectroscopy. J. Radioanal. Nucl. Chem. 276:639–643.

Wielopolski L., I. Orion, G. Hendrey, and H. Rogers. 2000. Soil carbon measurements using inelastic neutron scattering. IEEE Trans. Nucl. Sci. 47:914–917.

Wielopolski L., G. Hendrey, K. H. Johnsen, S. Mitra, S. A. Prior, H. H. Rogers, and H. A. Torbert. 2008. Nondestructive system for analyzing carbon in the soil. Soil Sci. Soc. Amer. J. 72(5):1269–1277.

Wielopolski L., R. D. Yanai, C. R. Levine, S. Mitra, and M. A. Vadeboncoeur. 2010. Rapid, nondestructive carbon analysis of forest soils using neutron-induced gamma-ray spectroscopy. For. Ecol. Manag. 260:1132–1137.

Wielopolski L., A. Chatterjee, S. Mitra, and R. Lal. 2011. *In situ* determination of soil carbon pool by inelastic neutron scattering: Comparison with dry combustion. Geoderma. 160:394–399.

APPENDIX

THEORETICAL MODEL OF GAMMA RAY YIELD IN INS MEASUREMENTS

Analysis shows that variation in soil carbon distribution affects the carbon-associated gamma peak. To theoretically estimate the effect of this variation, a mathematical model was developed to characterize the influence of soil carbon distribution on the 4.43-MeV gamma detector signal. The modeled INS system consists of a neutron source and detector on the soil surface at a distance "a" from one another (Fig. 1A). Using a cylindrical coordinate system whose origin coincides with the detector and the Z axis coinciding with the source-detector line, let us consider the elementary volume of soil $dV = r \cdot dr \cdot dz \cdot d\varphi$ that is situated at the point r, z, φ (i.e., r is the distance between axis Z and dV; z

is the distance from the origin to the intersection of r and axis Z; and φ is an angle between r and the soil surface) and contains $N_C \cdot dV$ carbon-12 nuclei (N_C is the number of carbon-12 nuclei per cm^3). Then the rate of 4.43-MeV gamma rays $n_\gamma \cdot dV$ caused by inelastic neutron scattering in the elemental volume dV can be estimated as:

$$n_\gamma \cdot dV = \sigma_c \cdot N_c \cdot \frac{\Phi_0 \cdot \exp(-\Sigma_s \cdot x)}{4\pi \cdot x^2} dV \quad (1A)$$

where σ_C is the cross section for carbon nucleus (cm^2), Φ_0 is a neutron flux (s^{-1}), x is the distance between the source and dV (cm), and Σ_S is the total macroscopic cross section of neutrons interacting with soil nucleus (cm^{-1}). Σ_S depends on soil content and, if the soil consists of i types of different nuclei, can be estimated as:

$$\Sigma_s = \Sigma \sigma_i \cdot \frac{N_A}{A_i} \cdot w_i \cdot \rho_s \quad (2A)$$

where σ_i is the cross section for the i_{th} type of nucleus in soil (cm^2), A_i is the atomic weight of this type of nucleus (g $mole^{-1}$), w_i is their mass portion in the soil, N_A is Avogadro number ($mole^{-1}$), and ρ_S is the soil density (g cm^{-3}).

The gamma flux from dV on the elementary area of the detector dS can be estimated as:

$$\frac{dN_\gamma}{dS} = n_\gamma \cdot \frac{\exp(-\mu_1 \cdot y)}{4\pi \cdot y^2} \cdot \sin\theta dV \quad (3A)$$

where y is the distance between dS and dV (cm), θ is the angle between y and the soil surface (rad) where sin θ can be estimated as r/y, and μ_1 is the linear attenuation coefficient of 4.43-MeV gamma rays in soil (cm^{-1}); μ_1 depends on soil content and, if the soil consists of the j type of element, can be estimated as

$$\mu_1 = \sum \mu_{m,j} \cdot w_j \cdot \rho_s \quad (4A)$$

where $\mu_{m,j}$ is the mass attenuation coefficient of the j_{th} type of soil element (cm^2 g^{-1}).

Total gamma ray flux N_γ (s cm^{-2}) from the semi-infinite layer of soil on the elementary surface of the detector can be estimated by integrating Eq.(4A) by volume as:

$$N_\gamma = \int_0^\infty \int_{-\infty}^\infty \int_0^\pi \frac{\exp(-\mu_1 \cdot y)}{4\pi \cdot y^2} \cdot \frac{r}{y} \cdot \sigma_c \cdot N_c \cdot \frac{\Phi_0 \cdot \exp(-\Sigma_s \cdot x)}{4\pi \cdot x^2} \cdot r \cdot \sin(\phi) dr \cdot dz \cdot d\varphi =$$

$$= \frac{\sigma_C \cdot \Phi_0}{16 \cdot \pi^2} \int_0^\infty \int_{-\infty}^\infty \int_0^\pi \frac{\exp(-\mu_1 \cdot y)}{y^3} \cdot N_C \cdot \frac{\exp(-\Sigma_s \cdot x)}{x^2} \cdot r^2 \cdot \sin(\phi) dr \cdot dz \cdot d\varphi \quad (5A)$$

The distances between dV and the detector (x) and between dV and the source (y) can be calculated as:

$$x = \sqrt{r^2 + (a+z)^2} \quad (6A)$$

$$y = \sqrt{r^2 + z^2} \quad (7A)$$

Eq.(5A) can be used to estimate the dependence of the gamma detector yield with different soil parameters (e.g., the weight percent of some type of nuclei, or soil density, or thickness of the soil layer, etc.).

The total macroscopic cross section of neutrons interacting with soil nucleus and the linear attenuation coefficient of 4.43 MeV gamma rays in soil was calculated by Eq.(2A) and Eq.(4A). The interaction cross section of 14 MeV neutrons with elemental C, Si-28, and O-16 nuclei and the mass attenuation coefficients of 4.43 MeV gamma rays for carbon, silicon, and oxygen for the calculations of these values are presented in Table 1A.

TABLE 1A. Mass Attenuation Coefficients of 4.43-MeV Gamma Rays and Interaction Cross Sections of 14-MeV Neutrons With Nuclei in Elemental Media (NIST, Gaithersburg, MD; NNDC, Brookhaven National Laboratory, Upton, NY)

		Elemental Media		
Parameter		**Carbon**	**Silicon**	**Oxygen**
μ_m, $cm^2 \cdot g^{-1}$		0.0285	0.031	0.0290
σ, barn	Nuclei	C elemental	Si-28	O-16
	Value	1.32	1.82	1.59

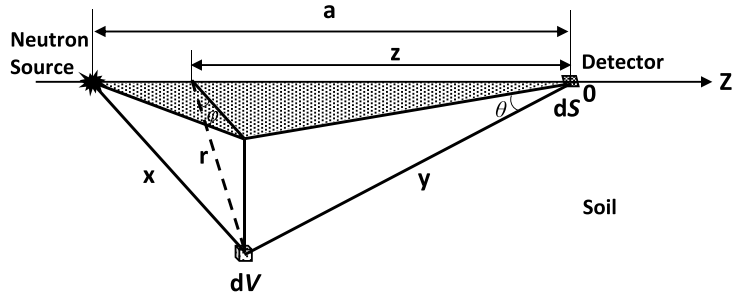

FIG. 1A. Diagram describing the model parameters incorporated into Eq.(5A).